Title: Effects of HFIR Neutron Irradiation on Fracture Toughness Properties of Standard and Ni-doped F82H

Authors: Xiang Chen [a,*], Mikhail A. Sokolov [a], Janet Robertson [a], Masami Ando [b], Josina W. Geringer [a], Hiroyasu Tanigawa [b], Yutai Katoh [a]

[a]Oak Ridge National Laboratory, PO Box 2008, Oak Ridge, TN 37831, USA

[b] National Institutes for Quantum and Radiological Science and Technology, Rokkasyo Fusion Institute, 2-166 Oaza-Obuchi-Aza-Omotedate, Rokkasho-mura, Kamikita-gun, Aomori 039-3212, Japan

[*]**Corresponding Author**: P.O. Box 2008, Building 4500S MS-6136, Oak Ridge, TN 37831-6136, USA, Tel: +1-865-574-5058, Fax: +1-865-241-3650, email: chenx2@ornl.gov

Abstract

F82H is the Japanese reference reduced-activation ferritic-martensitic (RAFM) steel for fusion blanket applications. The harsh environment of a fusion reactor, such as neutron irradiation and He/H damage, can result in significant degradation of F82H fracture toughness. Therefore, understanding the fracture toughness behavior of F82H in the fusion environment is critical to ensure the long-term safe operation of the fusion reactor. In this paper, we summarize seven irradiation campaigns of the High Flux Isotope Reactor (HFIR) at Oak Ridge National Laboratory (ORNL) covering five variants of F82H steels, including F82H IEA, F82H Mod3, F82H doped with 1.4% natural Ni, F82H doped with 1.4% ^{58}Ni, and F82H doped with 1.4% ^{60}Ni. The irradiation temperatures covered the range from 220 °C to 530 °C and the neutron irradiation dose spanned 4 dpa to 70 dpa. The effects of neutron irradiation temperature, dose, materials composition, Ni doping, and He production on F82H fracture toughness are discussed. Our results showed that irradiation embrittlement monotonically decreased with increasing irradiation temperature until 400 °C for F82H IEA and F82H Mod3. F82H Mod3 showed better fracture toughness than F82H IEA both before and after neutron irradiation. We determined that 1.4% Ni alloying can be applied to F82H for simulating He effect in a fission reactor without jeopardizing the fracture toughness of the material. However, more studies are needed to understand the effect of high dose (>20 dpa) and He production on F82H fracture toughness.

Keywords: Irradiation Embrittlement; Fracture Toughness; He Effect; Ni doping; Reduced Activation Ferritic-Martensitic Steel; F82H

1. Introduction

Reduced-activation ferritic-martensitic (RAFM) steel is the candidate structural material for fusion blanket applications [[1-[5]. It has favorable properties for fusion applications such as lower radioactivity, superior swelling resistance, good thermal conductivity, and sufficient fracture toughness in the normalized and tempered condition. However, the harsh environment of a fusion reactor, such as neutron irradiation and He/H damage, can result in significant degradation of fracture toughness. Therefore, understanding the fracture toughness behavior of RAFM steels in the fusion environment is critical to ensure the long-term safe operation of the fusion reactor. Due to the absence of dedicated fusion neutron sources, fission research reactors are usually used to irradiate RAFM steels. One drawback of such substitution is that the fission reactors cannot provide 14-MeV high energy neutrons as the fusion reactors and therefore some transmutation reaction products, such as He and H, cannot be reproduced. To simulate the He effect on top of the irradiation effect, RAFM steels are doped with isotopes of ^{10}B, ^{58}Ni, or ^{54}Fe [[2] to generate transmutation He in a fission reactor.

The Japanese reference RAFM steel, F82H (8Cr-2WVTa), was developed by JAERI and NKK corporation [[6]. Under the auspices of the International Energy Agency (IEA), two 5-ton ingots of F82H (IEA heats) were melted and made available for international collaborations between the EU, Japan, and the US. A toughness-improved F82H steel called F82H Mod3 has been developed with reduced Ti (<10 ppm) and N (<20 ppm) and increased Ta (0.1wt%) [[1]. Also, F82H doped with B or Ni has been studied to evaluate the He effect on materials properties [[7-[9].

The Master Curve (MC) method, fully described in the ASTM E1921 standard [[10], has been widely used to characterize the transition fracture toughness and irradiation-induced embrittlement in RAFM steels [[11-[20]. The method allows testing a relatively small number of specimens to determine the median toughness vs. temperature curve. The method applies the statistical weakest-link theory to model specimen size effects and size-adjust fracture toughness results from various size specimens to reference 1T (one-inch thickness) specimens. However, research has indicated that for RAFM steels and especially when testing is performed on sub-size specimens, other factors, such as loss of the constraint, the shape of the MC, and the statistical size effect [[21-[26], may need to be taken into account. Nonetheless, the standard MC method facilitates the characterization and comparison of RAFM steel fracture toughness properties among the fusion research community.

Since 1997, more than seven irradiation campaigns in the High Flux Isotope Reactor (HFIR) at Oak Ridge National Laboratory (ORNL) have included F82H to study the material irradiation response. The irradiation temperatures covered the range from 220 °C to 530 °C and the neutron irradiation dose spanned 4 to 70 displacements per atom (dpa). In this paper, we summarize previous MC fracture toughness results along with the latest results from two high dose irradiation capsules. The effects of neutron irradiation temperature, dose, material composition, Ni doping, and He production on F82H fracture toughness are discussed. Results will also be compared with literature data of irradiation embrittlement in RAFM steels.

2. Experimental

2.1 Materials

F82H steels investigated in this study include F82H IEA heat, F82H Mod3, F82H doped with 1.4% natural Ni, F82H doped with 1.4% ^{58}Ni, and F82H doped with 1.4% ^{60}Ni. The compositions of these steels are listed in Table 1 [[27, [28] and Table 2 summarizes the heat treatment conditions for these materials. Based on the work of Sawai et al. [[28],1.4% Ni doping and the applied heat treatment condition didn't cause apparent modification of unirradiated steel microstructure. No delta-ferrite or retained austenite was observed in the metallographic examination. In addition, room temperature yield strength and microhardness results for 1.4% Ni-doped F82H are within the scatter band of those values for F82H-IEA based on our tests. For F82H doped with natural Ni or ^{58}Ni, both the He effect (^{58}Ni(n, γ)^{59}Ni followed by ^{59}Ni(n, α)^{56}Fe reaction) and the Ni alloying effect are investigated. For F82H doped with ^{60}Ni, only the Ni alloying effect is investigated. For irradiation in the HFIR flux trap positions (target positions at the center of the reactor core and surrounded by two concentric fuel elements [[29]), the He production rates for various F82H materials are summarized in Table 3 based on values reported in Refs. [[28, [30-[33].

2.2 Irradiation Conditions

Fracture toughness specimens in seven irradiation campaigns in HFIR, denominated RB11J, RB12J, JP25, JP26, JP27, JP28, and JP29, are covered in this study. The timeline and target irradiation conditions are shown in Figure 1. The RB11J and RB12J capsules were irradiated in the HFIR removable beryllium positions with europium oxide (Eu_2O_3) thermal neutron shields for neutron spectrum tailoring. The JP capsules were full-length target capsules irradiated in the HFIR flux trap positions. Irradiation temperatures were measured by thermocouples for the RB capsules and by SiC thermometry specimens for all the JP capsules using the algorithm and methods described by Campbell et al. [[34].

2.3 Specimens

The fracture toughness specimen geometry, size, and orientation are illustrated in Figure 2. The orientation follows the crack plane identification in the ASTM E399 standard [[35], i.e., the first letter designates the direction normal to the crack plane and the second letter designates the expected direction of crack propagation. The specimen size has significantly decreased throughout seven irradiation campaigns due to the development of small specimen testing techniques. In RB11J and RB12J, both 0.18T disk compact tension (DCT) specimens (4.6 mm thickness and 12.5 mm diameter) and 1/3-size precracked Charpy V-notch (PCCVN) bend bar specimens (3.3 × 3.3 × 25.4 mm^3) were used. In JP25, only 1/3-size PCCVN specimens were used. In JP26, specimen size was further reduced and half-thickness 1/3-size PCCVN bend bar specimens (1.65 × 3.3 × 25.4 mm^3) were used. In JP27-JP29 irradiation campaigns, a new miniature multi-notch bend bar specimen (referred to as MxCVN hereafter with x being the number of notches), specifically developed within the ORNL Fusion Materials Program [[36], was used. The MxCVN specimen has a dimension of 1.65 mm thickness, 3.3 mm width, and 9*(x+1) mm length. Despite its small size, the MxCVN specimen follows the same size ratio of a bend bar specimen in the ASTM E1921 standard. Due to shared loading portions between neighboring notches, the MxCVN specimen consumes significantly less material than a standard single notch bend bar specimen and is beneficial for post-irradiation evaluation. Before irradiation, all fracture toughness specimens were fatigue precracked to a crack size to width (a/W) ratio of ~0.5.

2.4 Method

We performed fracture toughness testing and analysis according to the MC method in the ASTM E1921 standard. Two factors were considered in determining the test temperatures. The first factor is that the testing temperature should not be too high such that the measured fracture toughness is within the fracture toughness capacity limit $K_{Jclimit}$ given in Eq. (1):

$$K_{Jc\lim it} = \sqrt{\frac{Eb_o \sigma_{YS}}{30(1-\nu^2)}} \quad (1)$$

where:

E = Young's modulus at the test temperature,

b_0 = initial uncracked ligament length,

σ_{YS} = material yield strength at the test temperature,

v = Poisson's ratio.

The second factor is that the testing temperatures should not be more than 50 °C lower than the MC reference temperature as required in ASTM E1921. Therefore, the test temperatures were selected as a compromise between obtaining as high fracture toughness results as possible and still within the fracture toughness capacity limit for most specimens.

Upon completion of testing, the crack size was measured on the fracture surface. The elastic-plastic equivalent stress intensity factor, K_{Jc}, was derived from the J-integral at the onset of cleavage fracture and size-adjusted to 1T based on the statistical weakest-link theory:

$$K_{Jc(1T)} = 20 + [K_{JC(o)} - 20](\frac{B_0}{B_{1T}})^{1/4} \quad (2)$$

where:

$K_{Jc(1T)}$ = K_{Jc} for a specimen thickness of one inch (B_{1T}=25.4 mm),

$K_{Jc(o)}$ = K_{Jc} for a specimen thickness of B_o.

We then calculated the MC provisional reference temperature T_{oq} using the multi-temperature analysis method in Eq. (3) and K_{Jc} data were censored against both the fracture toughness capacity limit $K_{Jclimit}$ and the slow stable crack growth limit $K_{Jc\Delta a}$ which equals the highest uncensored K_{Jc} in the data set obtained at any specimen size and test temperature when tests terminate in cleavage after slow stable crack growth exceeding the smaller of either $0.05b_0$ or 1 mm.

$$\sum_{i=1}^{N} \delta_i \frac{\exp[0.019(T_i - T_{oq})]}{11.0 + 76.7\exp[0.019(T_i - T_{oq})]} - \sum_{i=1}^{N} \frac{(K_{Jc(i)} - 20)^4 \exp[0.019(T_i - T_{oq})]}{\{11.0 + 76.7\exp[0.019(T_i - T_{oq})]\}^5} = 0 \quad (3)$$

where:

N = number of specimens tested,

T_i = test temperature corresponding to $K_{Jc(i)}$,

$K_{Jc(i)}$ = either a valid K_{Jc} datum or a datum replaced with a censoring value,

δ_i = 1.0 if the datum is valid or zero if the datum is a censored value,

T_{oq} = MC provisional reference temperature obtained by iteration.

Furthermore, the toughness-temperature curve can be derived using the following equation:

$$K_{Jc(med)} = 30 + 70\exp[0.019(T - T_{oq})] \tag{4}$$

where:

$K_{Jc(med)}$ = median fracture toughness at temperature T for 1T size specimen,

3. Results

3.1 RB11J and RB12J

F82H IEA in both T-L and L-T orientations was irradiated in RB11J and RB12J [[17, [37]. The target irradiation temperatures were 300 °C and 500 °C and the actual irradiation temperatures were measured by thermocouples. Figure 3 summarizes the MC results of the material. For the unirradiated condition, F82H IEA showed orientation dependence for fracture toughness with the MC reference temperature T_0 equaling -68 °C for the T-L orientation and -109 °C for the L-T orientation. In addition, a significant irradiation temperature effect on embrittlement was observed for both orientations. For 0.18T DCT specimens in the T-L orientation, irradiation at a lower temperature range of 221 °C – 280 °C to 3.8 dpa resulted in 191 °C upward shift in T_0 as compared with 57 °C upward shift in T_0 when materials were irradiated at a higher temperature range of 349 °C – 405 °C. For 1/3-size PCCVN specimens in the L-T orientation, irradiation at a lower temperature range of 275 °C – 313 °C to 4.8 dpa resulted in 103 °C upward shift in T_0 as compared with 42 °C upward shift in T_0 when materials were irradiated at a higher temperature range of 467 °C – 531 °C.

3.2 JP25

The 1/3-size PCCVN specimens of F82H IEA in the L-T orientation were irradiated in JP25 to 17.5 dpa [[17]. The target irradiation temperature was 300 °C although the actual irradiation temperature, measured by the SiC thermometry specimen, was approximately 380 °C. Figure 4 shows the MC results of the material. Neutron irradiation at 380 °C to 17.5 dpa resulted in an upward shift of 109 °C in the MC reference temperature T_0.

3.3 JP26

Half-thickness 1/3-size PCCVN specimens of both F82H IEA and F82H+1.4% natural Ni in the T-S orientation were irradiated in JP26 to a dose range of 6 dpa – 8 dpa [[21, [38]. The irradiation temperatures were targeting 300 °C, 400 °C, and 500 °C and were confirmed by SiC thermometry specimens. Figure 5 shows the MC results of the two materials. For F82H IEA, an irradiation temperature effect on embrittlement was observed. With the irradiation temperature increasing from 300 °C to 500 °C, the upward shift in MC reference T_0 decreased from 141 °C to 74 °C. A similar trend was also observed in F82H+1.4% natural Ni, i.e., ΔT_0 of 163 °C for irradiation at 300 °C vs. ΔT_0 of 72 °C for irradiation at 500 °C. F82H+1.4% natural Ni showed slightly enhanced irradiation embrittlement when irradiated at 300 °C, but not at 500 °C.

3.4 JP27

M3CVN specimens of F82H IEA, F82H Mod3, F82H+1.4% ^{58}Ni, and F82H+1.4% ^{60}Ni in the T-S orientation were irradiated in JP27 to a peak dose of 22 dpa [[38]. The target irradiation temperatures were 300 °C and 400 °C and were confirmed by SiC thermometry specimens. Figure 6 illustrates the MC results of all four F82H variants. An irradiation temperature effect, manifested by a larger upward shift in MC reference temperature T_0 for irradiations at 300 °C compared with irradiations at 400 °C, was observed in all materials. F82H Mod3 exhibited less embrittlement than F82H IEA for both irradiation temperatures. In comparison with F82H IEA, Ni-doped F82H showed similar embrittlement for irradiation at 300 °C, whereas less embrittlement was observed in Ni-doped F82H for irradiation at 400 °C.

3.5 JP28 and JP29

M3CVN specimens of F82H IEA, F82H Mod3, F82H+1.4% ^{58}Ni, and F82H+1.4% ^{60}Ni in the T-S orientation were irradiated in JP28 and JP29 to a peak dose of 70 dpa. The target irradiation temperature was 300 °C although the actual irradiation temperatures, measured by the SiC thermometry specimens, were approximately 342 °C for F82H IEA and F82H Mod3 and 317 °C for F82H+1.4% ^{58}Ni and F82H+1.4% ^{60}Ni. Figure 7 illustrates the MC results of all materials. F82H+1.4% ^{58}Ni exhibited the largest increase in MC reference temperature T_0 (+161 °C) among all tested materials whereas F82H Mod3 showed the least increase in T_0 (+28 °C). For F82H doped with 1.4% ^{60}Ni, the upward shift in T_0 (+29 °C) was less than that in F82H IEA (+55 °C), indicating no detrimental effect of 1.4% ^{60}Ni doping for this test condition.

4. Discussion

The effect of irradiation temperature and dose on the fracture toughness of F82H IEA and F82H Mod3 is summarized in Figure 8. The irradiation temperature had a significant effect on irradiation embrittlement for both materials. The irradiation embrittlement monotonically decreased with the increase in the irradiation temperature until the irradiation temperature reached 400 °C. However, the 342 °C/68-dpa irradiation for F82H IEA and F82H Mod 3 showed much less embrittlement than what would be expected for irradiation around 300 °C and was close to the 400 °C irradiation case. This indicates that specimens potentially experienced a higher irradiation temperature which was not captured by the SiC thermometry specimen. While the exact cause for the higher irradiation temperature has not been determined yet, potential causes include machining errors of the irradiation capsule or errors during the assembly of the irradiation capsule. For both cases, if the heat transfer from specimens (heat generated by gamma heating) to the reactor coolant was hindered and deviated from the design value, a high irradiation temperature would be expected. However, why the potentially high irradiation temperature was not captured by the SiC thermometry specimen remains a myth. Indeed, we compared the irradiation embrittlement between JP27 and JP28/29 for F82H IEA, F82H Mod3, F82H+1.4% ^{58}Ni, and F82H+1.4% ^{60}Ni s in Figure 9. Despite much higher irradiation dose in JP28/29 than in JP27, four F82H variants irradiated in JP28/29 at 317 °C and 342 °C showed irradiation embrittlement similar to the same materials irradiated in JP27 at 400 °C except for F82H+1.4% ^{58}Ni which may be due to the additional helium effect and will be discussed further below. Additional microstructure study is needed to elucidate the observation. Comparing post-irradiation fracture toughness between F82H IEA and F82H Mod3, we found that F82H Mod3 showed less embrittlement than F82H IEA. Therefore, the improved fracture toughness of F82H Mod3 was retained even after irradiation. In terms of the effect of irradiation dose on embrittlement, no saturation effect on F82H IEA embrittlement was observed up to 20 dpa. As shown in Figure 8, two fitting trend lines, defined in Eq. (5) [[40], are used to describe F82H IEA general irradiation embrittlement behaviors at 300 °C and 400 °C:

$$\Delta T_0 = A[1-\exp(-\frac{dose}{\tau})] \quad (5)$$

where A and τ are fitting constants. Unfortunately, the fracture toughness result of F82H IEA after 68 dpa irradiation was clouded by the uncertainty in the irradiation temperature. Hence, we cannot verify if the trend curve gives a satisfactory prediction of the F82H IEA embrittlement behavior for irradiation dose higher than 20 dpa.

A comparison of irradiation embrittlement between this study and literature for F82H IEA and Eurofer97 is shown in Figure 10 [[19, [23, [24, [39, [40]. Eurofer97 (nominal composition Fe-9Cr-1.1W-0.2V-0.12Ta) is the European reference RAFM steel for the first wall and blanket applications of the DEMO fusion reactor [[41-[43] and has been frequently compared with F82H. This study covers a wider range of irradiation doses than literature data (18 dpa vs. ~9 dpa). Literature data show a similar degree of embrittlement between F82H IEA and Eurofer97 for irradiation around 290 °C – 300 °C up to 5 dpa, whereas we found slightly less embrittlement for F82H IEA in our study. Considering the complexity of neutron irradiation tests and different research reactors used in these studies, the difference is still considered as small and our results are line with literature data.

To evaluate the Ni alloying and He effects on irradiation embrittlement of F82H, the upward shift in the MC reference temperature T_0 for Ni-doped F82H is compared with F82H IEA in Figure 11 for three irradiation temperatures, i.e., 300 °C – 342 °C, 400 °C, and 500 °C. For F82H doped with 1.4% ^{60}Ni where only the Ni alloying effect was active, the irradiation embrittlement was either similar or less than that of F82H IEA when the material was irradiated between 300 °C to 400 °C for all the investigated dose levels. The T_0 of F82H +1.4% ^{60}Ni in the unirradiated condition was also similar to that of F82H IEA (-99 °C vs. -102 °C). Therefore, we did not observe any detrimental effect of 1.4% ^{60}Ni alloying on F82H MC fracture toughness, which was not reported previously. For F82H doped with 1.4% natural Ni or 1.4% ^{58}Ni, the He production rate in HFIR flux trap positions was approximately 7 appm/dpa or 11 appm/dpa, respectively. The irradiation conditions in this study covered a He production range from 48 appm to 770 appm. Except for F82H+1.4% ^{58}Ni irradiated at 300 °C – 342 °C to 70 dpa corresponding to ~770 appm He production, F82H doped with 1.4% natural Ni or 1.4% ^{58}Ni showed similar or less embrittlement than the standard F82H IEA for the other irradiation conditions. At the highest He production level, significantly more embrittlement was observed in F82H+1.4% ^{58}Ni than F82H IEA. This observation is in agreement with the study of Yamamoto et al. [[44] that the contribution of He to embrittlement appears to emerge at higher He concentrations, estimated to be above 400 appm to 600 appm. In the work of Wakai et al. [[7], they applied B doping in F82H for He production and observed upward shifts in ductile-to-brittle transition temperatures (DBTT) at much lower He levels (190 appm – 330 appm). However, the upward shift in DBTT occurred when materials were irradiated at 250 °C and the shift decreased when the irradiation temperature increased to 300 °C. Therefore, their results are not conclusive in determining the threshold He levels for additional embrittlement. In addition, their results seem to indicate there is an additional temperature effect on the He embrittlement for F82H. Tanigawa et al. [[33] also studied the He effect on Charpy impact properties of F82H by irradiating F82H doped with 2% natural Ni in HFIR. Compared with F82H IEA, F82H+2% natural Ni exhibited a larger shift in DBTT when the material was irradiated at 300 °C to 5 dpa corresponding to 50 appm He production. However, the same Ni-doped F82H showed less embrittlement than F82H IEA when the irradiation temperatures were between 380 °C and 500 °C for irradiation doses up to 20 dpa corresponding to 200 appm He production. Therefore, a clear threshold value for the detrimental He effect could not be established and the same potential temperature effect on the He embrittlement was observed in that study. In addition, the 2% natural Ni lowered the Ac1 temperature (lowest temperature at which austenite can form on heating at a specified heating rate) of F82H and the tempering heat treatment (750 °C/1hr) applied in the work of Tanigawa et al. [[33] would result in both fresh and tempered martensites based on the study of Sawai et al. [[28]. Therefore, the difference in the starting microstructures between F82H doped with 2% natural Ni and F82H IEA further clouded the He effect on ΔDBTT.

4. Conclusions

Burning questions remain for the irradiation embrittlement behavior of F82H. For example, at what dose levels does the irradiation embrittlement saturate and is the saturation dose temperature-dependent? In addition, what is the threshold value for the detrimental He effect on material fracture toughness and is it temperature-dependent? Last but not least, how much Ni alloying can be applied to F82H to simulate the He effect with fission neutron sources without jeopardizing the microstructure and properties of the material? In this study, we attempted to tackle these questions with some success by evaluating the effects of neutron irradiation on the fracture toughness properties of F82H IEA, F82H Mod3, F82H+1.4% natural Ni, F82H+1.4% ^{58}Ni, and F82H+1.4% ^{60}Ni. The irradiation temperatures covered the range from 220 °C to 530 °C and the neutron irradiation dose spanned 4 dpa to 70 dpa. The main findings of this study include:

1) The irradiation temperature had a significant effect on irradiation embrittlement for F82H IEA and F82H Mod3. The irradiation embrittlement monotonically decreased with increasing irradiation temperature until the irradiation temperature reached 400 °C;

2) Higher dose resulted in more embrittlement in F82H IEA, which did not saturate up to 20 dpa. More studies are needed to find if there is a saturation effect of the irradiation dose on F82H embrittlement;

3) F82H Mod3 showed better fracture toughness than F82H IEA both before and after neutron irradiation;

4) 1.4% Ni alloying can be applied to F82H for simulating the He effect in a fission reactor. We did not observe any detrimental effect of 1.4% ^{60}Ni alloying on F82H fracture toughness, both before and after neutron irradiation;

5) Compared with F82H IEA, we observed significantly more embrittlement in F82H+1.4% ^{58}Ni irradiated at 300 °C – 342 °C to 70 dpa corresponding to ~770 appm He production. However, our current data are not sufficient to pin down accurately the threshold He content for additional embrittlement. In addition, we cannot exclude the possibility that irradiation temperatures also play a role in determining such threshold value.

Acknowledgments

This study was supported by the U.S. Department of Energy, Office of Fusion Energy Sciences and the National Institutes for Quantum and Radiological Science and Technology (QST) under contract DE-AC05-00OR22725 with Oak Ridge National Laboratory (ORNL) managed by UT Battelle, LLC. A portion of this research at ORNL's High Flux Isotope Reactor was sponsored by the Scientific User Facilities Division, Office of Basic Energy Sciences, US Department of Energy. The authors would like to thank Eric Manneschmidt and Ronald Swain from ORNL for performing part of mechanical testing in this study. Besides, we are grateful for the hot cell testing support from the ORNL Irradiated Materials Examination and Testing Facility (IMET) team.

Reference

[1] K. Shiba, H. Tanigawa, T. Hirose, T. Nakata, Development of the toughness-improved reduced-activation F82H steel for DEMO reactor, Fusion Science and Technology 62(1) (2012) 145-149.

[2] L. Tan, Y. Katoh, A.-A. Tavassoli, J. Henry, M. Rieth, H. Sakasegawa, H. Tanigawa, Q. Huang, Recent status and improvement of reduced-activation ferritic-martensitic steels for high-temperature service, Journal of Nuclear Materials 479 (2016) 515-523.

[3] K. Shiba, M. Enoeda, S. Jitsukawa, Reduced activation martensitic steels as a structural material for ITER test blanket, Journal of nuclear materials 329 (2004) 243-247.

[4] S. Jitsukawa, M. Tamura, B. Van der Schaaf, R. Klueh, A. Alamo, C. Petersen, M. Schirra, P. Spaetig, G. Odette, A. Tavassoli, Development of an extensive database of mechanical and physical properties for reduced-activation martensitic steel F82H, Journal of Nuclear Materials 307 (2002) 179-186.

[5] A.-A. Tavassoli, J.-W. Rensman, M. Schirra, K. Shiba, Materials design data for reduced activation martensitic steel type F82H, Fusion Engineering and Design 61 (2002) 617-628.

[6] K. Shiba, A. Hishinuma, A. Tohyama, K. Masamura, Properties of low activation ferritic steel F82H IEA heat. Interim report of IEA round-robin tests. 1, Japan Atomic Energy Research Inst., 1997.

[7] E. Wakai, S. Jitsukawa, H. Tomita, K. Furuya, M. Sato, K. Oka, T. Tanaka, F. Takada, T. Yamamoto, Y. Kato, Radiation hardening and-embrittlement due to He production in F82H steel irradiated at 250° C in JMTR, Journal of nuclear materials 343(1-3) (2005) 285-296.

[8] N. Okubo, E. Wakai, S. Matsukawa, K. Furuya, H. Tanigawa, S. Jitsukawa, Heat treatment effects on microstructures and DBTT of F82H steel doped with boron and nitrogen, Materials transactions 46(2) (2005) 193-195.

[9] M. Sokolov, Results of fracture toughness tests of several RAFM steels irradiated in JP-27 capsule in HFIR, Fusion Materials Semiannual Progress Report, DOE-ER-0313/45 (2009) 49-51.

[10] ASTM E1921-19b, Standard Test Method for Determination of Reference Temperature, To, for Ferritic Steels in the Transition Range, ASTM International, West Conshohocken, PA, 2019, www.astm.org

[11] W. Han, K. Yabuuchi, R. Kasada, A. Kimura, E. Wakai, H. Tanigawa, P. Liu, X. Yi, F. Wan, Application of small specimen test technique to evaluate fracture toughness of reduced activation ferritic/martensitic steel, Fusion Engineering and Design 125 (2017) 326-329.

[12] B.J. Kim, R. Kasada, A. Kimura, E. Wakai, H. Tanigawa, Application of master curve method to the evaluation of fracture toughness of F82H steels, Journal of Nuclear Materials 442(1-3) (2013) S38-S42.

[13] B.J. Kim, R. Kasada, A. Kimura, H. Tanigawa, Evaluation of grain boundary embrittlement of phosphorus added F82H steel by SSTT, Journal of nuclear materials 421(1-3) (2012) 153-159.

[14] B.J. Kim, R. Kasada, A. Kimura, H. Tanigawa, Specimen Size Effects on Fracture Toughness of F82H Steel for Fusion Blanket Structural Material, Zero-Carbon Energy Kyoto 2010, Springer2011, pp. 286-291.

[15] B.J. Kim, R. Kasada, A. Kimura, H. Tanigawa, Effects of specimen size on fracture toughness of phosphorous added F82H steels, Fusion engineering and design 86(9-11) (2011) 2403-2408.

[16] M. Sokolov, A. Kimura, H. Tanigawa, S. Jitsukawa, Fracture toughness characterization of JLF-1 steel after irradiation in HFIR to 5 dpa, Journal of nuclear materials 367 (2007) 644-647.

[17] M. Sokolov, H. Tanigawa, G. Odette, K. Shiba, R. Klueh, Fracture toughness and Charpy impact properties of several RAFMS before and after irradiation in HFIR, Journal of nuclear materials 367 (2007) 68-73.

[18] M. Sokolov, H. Tanigawa, Application of the master curve to inhomogeneous ferritic/martensitic steel, Journal of nuclear materials 367 (2007) 587-592.

[19] E. Lucon, R. Chaouadi, M. Decréton, Mechanical properties of the European reference RAFM steel (EUROFER97) before and after irradiation at 300° C, Journal of nuclear materials 329 (2004) 1078-1082.

[20] E. Lucon, M. Decréton, E. van Walle, Mechanical characterization of EUROFER97 irradiated (0.32 dpa, 300° C), Fusion engineering and design 69(1-4) (2003) 373-377.

[21] T. Yamamoto, G. Odette, M. Sokolov, On the fracture toughness of irradiated F82H: Effects of loss of constraint and strain hardening capacity, Journal of nuclear materials 417(1-3) (2011) 115-119

[22] P. Mueller, P. Spätig, 3D finite element and experimental study of the size requirements for measuring toughness on tempered martensitic steels, Journal of nuclear materials 389(3) (2009) 377-384.

[23] T. Yamamoto, G. Odette, D. Gragg, H. Kurishita, H. Matsui, W. Yang, M. Narui, M. Yamazaki, Evaluation of fracture toughness master curve shifts for JMTR irradiated F82H using small specimens, Journal of nuclear materials 367 (2007) 593-598.

[24] P. Spätig, R. Bonadé, G. Odette, J. Rensman, E. Campitelli, P. Mueller, Plastic flow properties and fracture toughness characterization of unirradiated and irradiated tempered martensitic steels, Journal of nuclear materials 367 (2007) 527-538.

[25] G. Odette, T. Yamamoto, H. Kishimoto, M. Sokolov, P. Spätig, W. Yang, J.-W. Rensman, G. Lucas, A master curve analysis of F82H using statistical and constraint loss size adjustments of small specimen data, Journal of nuclear materials 329 (2004) 1243-1247.

[26] G. Odette, H. Rathbun, J. Rensman, F. Van Den Broek, On the transition toughness of two RA martensitic steels in the irradiation hardening regime: a mechanism-based evaluation, Journal of nuclear materials 307 (2002) 1011-1015.

[27] N. Okubo, M.A. Sokolov, H. Tanigawa, T. Hirose, S. Jitsukawa, T. Sawai, G. Odette, R. Stoller, Heat treatment effect on fracture toughness of F82H irradiated in HFIR, Journal of nuclear materials 417(1-3) (2011) 112-114.

[28] T. Sawai, M. Ando, E. Wakai, K. Shiba, S. Jitsukawa, Ni-doped F82H to investigate He effects in HFIR irradiation, Fusion science and technology 44(1) (2003) 201-205.

[29] High Flux Isotope Reactor (HFIR) USER GUIDE: A guide to in-vessel irradiations and experiments, revision 2.0, ORNL, November 2015, https://neutrons.ornl.gov/sites/default/files/High%20Flux%20Isotope%20Reactor%20User%20Guide%202.0.pdf

[30] L.R. Greenwood, B. D. Pierson, M. G. Cantaloub, and T. Trang-Le, Neutron Fluence Measurements and Radiation Damage Calculations for the JP28 And JP29 Experiments in HFIR, Fusion Materials Semiannual Progress Report, DOE-ER-0313/68 (2020).

[31] T. Hirose, Y. Katoh, H. Tanigawa, K.G. Field, H. Sakasegawa, B.K. Kim, M. Ando, D.T. Hoelzer, L. Tan, L.L. Snead, R.E. Stoller, Effects of High Dose Neutron Irradiation on Reduced-

activation Ferritic/Martensitic Steels, 17th International Conference on Fusion Reactor Materials, October 11-16, 2015, Aachen, Germany.

[32] R. Klueh, M. Sokolov, K. Shiba, Y. Miwa, J. Robertson, Embrittlement of reduced-activation ferritic/martensitic steels irradiated in HFIR at 300° C and 400° C, Journal of nuclear materials 283 (2000) 478-482.

[33] H. Tanigawa, K. Shiba, M. Sokolov, R. Klueh, Charpy impact properties of reduced-activation ferritic/martensitic steels irradiated in HFIR up to 20 dpa, Fusion science and technology 44(1) (2003) 206-210.

[34] A.A. Campbell, W.D. Porter, Y. Katoh, L.L. Snead, Method for analyzing passive silicon carbide thermometry with a continuous dilatometer to determine irradiation temperature, Nuclear Instruments and Methods in Physics Research Section B: Beam Interactions with Materials and Atoms 370 (2016) 49-58.

[35] ASTM E399-20, Standard Test Method for Linear-Elastic Plane-Strain Fracture Toughness of Metallic Materials, ASTM International, West Conshohocken, PA, 2020, www.astm.org

[36] X. Chen, M.A. Sokolov, Y. Katoh, M. Rieth, L.N. Clowers, Master Curve fracture toughness characterization of Eurofer97 using miniature multi-notch bend bar specimens for fusion applications, Proceedings of the ASME 2018 Pressure Vessels and Piping Conference, July 15-20, 2018, Prague, Czech Republic, PVP2018-85065.

[37] M.A. Sokolov, R.L. Klueh, G.R. Odette, K. Shiba, H. Tanigawa, Fracture toughness characterization of irradiated F82H in the transition region, Effects of Radiation on Materials: 21st International Symposium, ASTM International, 2004.

[38] M. Sokolov, G. Odette, T. Yamamoto, H. Tanigawa, N. Okubo, Dose dependence of fracture toughness of F82H steel, Fusion Materials Semiannual Progress Report, DOE-ER-0313/48 (2010) 46-49.

[39] J. Rensman, J. Van Hoepen, J. Bakker, R. Den Boef, F. Van Den Broek, E. Van Essen, Tensile properties and transition behaviour of RAFM steel plate and welds irradiated up to 10 dpa at 300 C, Journal of nuclear materials 307 (2002) 245-249.

[40] E. Gaganidze, Assessment of Fracture Mechanical Experiments on Irradiated EUROFER97 and F82H Specimens, Final Report for Task TW5-TTMS, 2007, pp. 001-D14.

[41] A. Kohyama, A. Hishinuma, D. Gelles, R. Klueh, W. Dietz, K. Ehrlich, Low-activation ferritic and martensitic steels for fusion application, Journal of Nuclear Materials 233 (1996) 138-147.

[42] P. Fernández, A. Lancha, J. Lapeña, M. Hernández-Mayoral, Metallurgical characterization of the reduced activation ferritic/martensitic steel Eurofer'97 on as-received condition, Fusion Engineering and Design 58 (2001) 787-792.

[43] N. Baluc, D. Gelles, S. Jitsukawa, A. Kimura, R. Klueh, G. Odette, B. Van der Schaaf, J. Yu, Status of reduced activation ferritic/martensitic steel development, Journal of Nuclear Materials 367 (2007) 33-41.

[44] T. Yamamoto, G.R. Odette, H. Kishimoto, J.-W. Rensman, P. Miao, On the effects of irradiation and helium on the yield stress changes and hardening and non-hardening embrittlement of~ 8Cr tempered martensitic steels: compilation and analysis of existing data, Journal of nuclear materials 356(1-3) (2006) 27-49.

Figures

Figure 1 Timeline and target irradiation conditions for F82H in HFIR

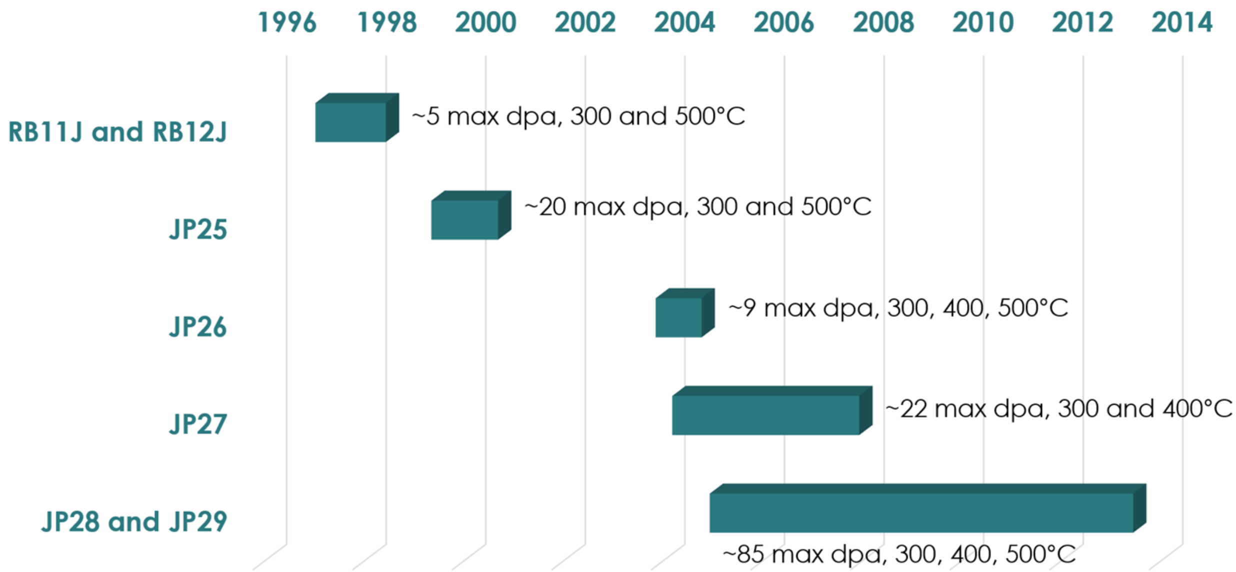

Figure 2 Fracture toughness specimen geometry, size, and orientation (L: longitudinal direction, T: long transverse direction, S: short transverse direction)

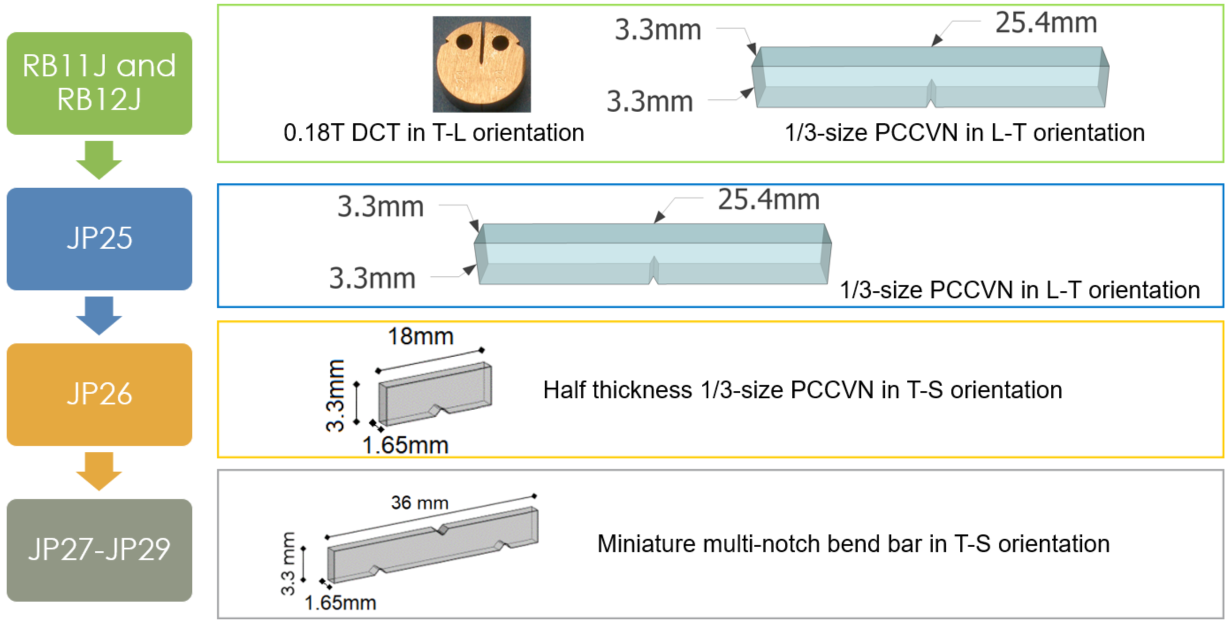

Figure 3 MC results of F82H IEA in RB11J and RB12J [[17,[37]. (a) 0.18T DCT in the T-L orientation, (b) 1/3-size PCCVN in the L-T orientation

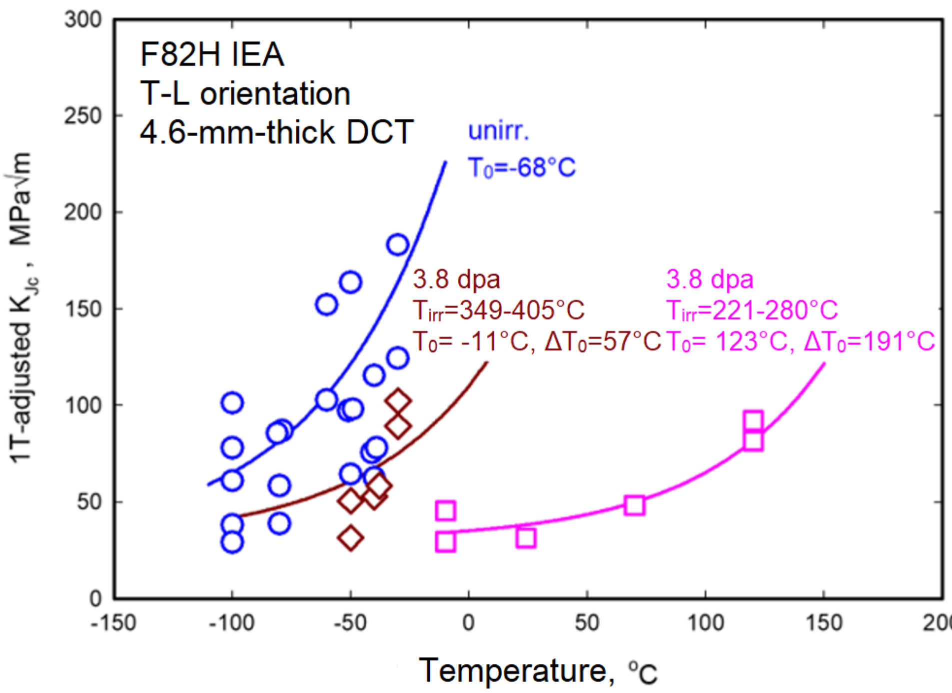

(a)

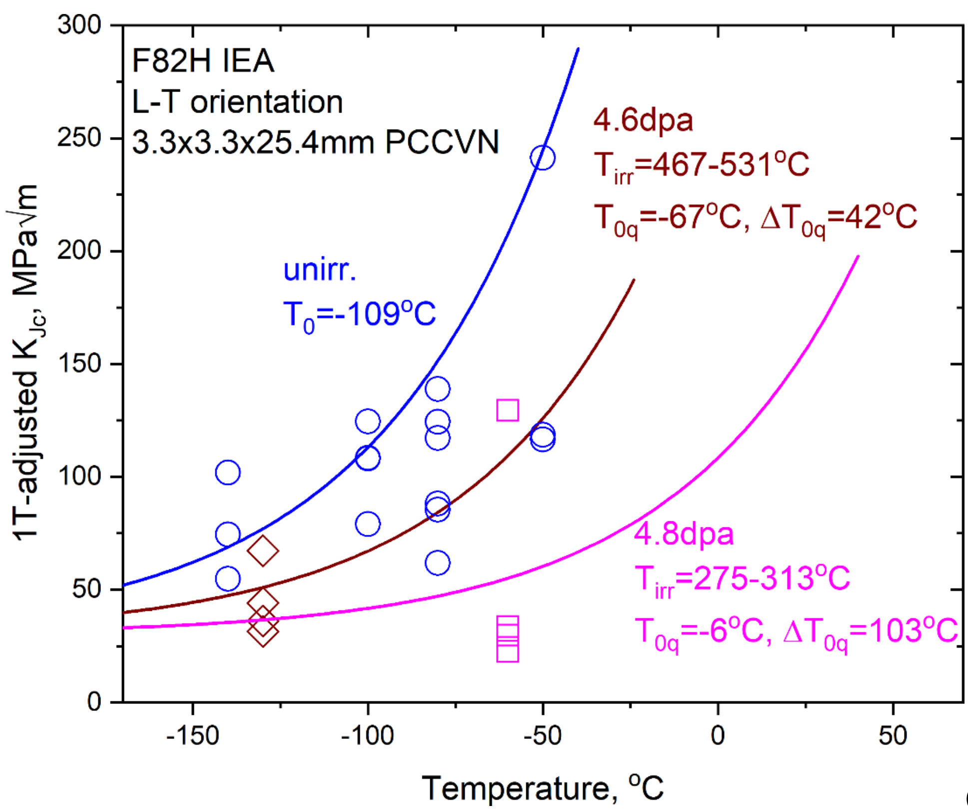

(b)

Figure 4 MC results of F82H IEA in JP25 [[17]

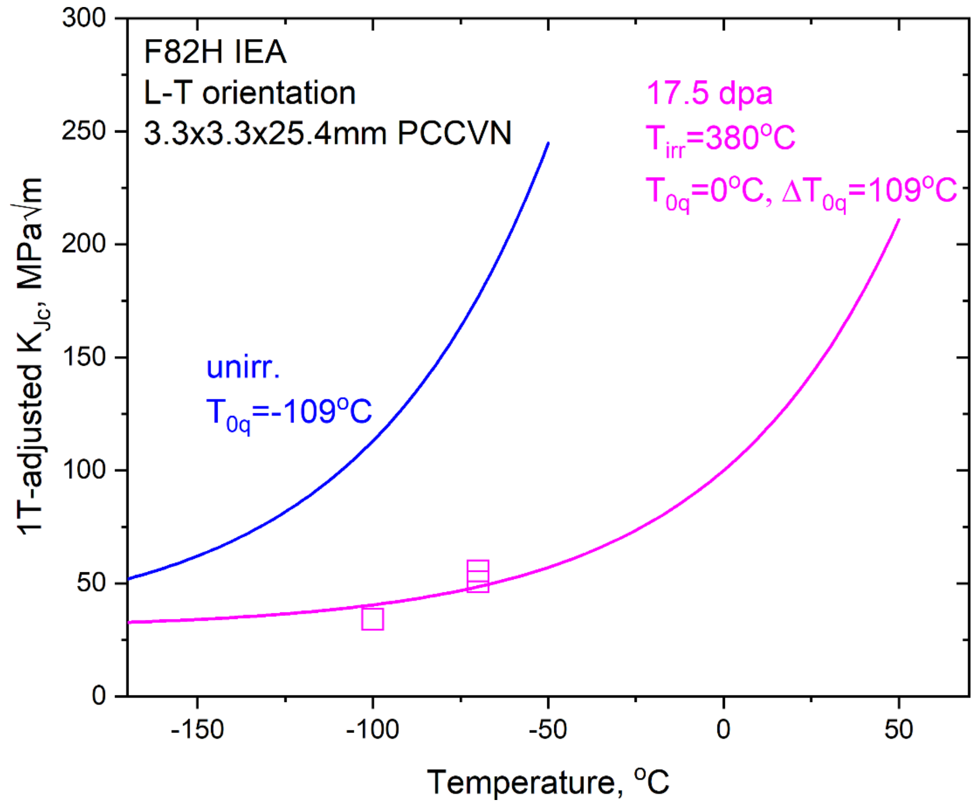

Figure 5 JP26 MC results for F82H IEA in (a) and F82H+1.4% natural Ni in (b) [[21, [38]. Note that unirradiated fracture toughness of F82H+1.4% natural Ni was not available during the preparation of this manuscript. Therefore, unirradiated fracture toughness of F82H+1.4% ^{58}Ni was used in (b).

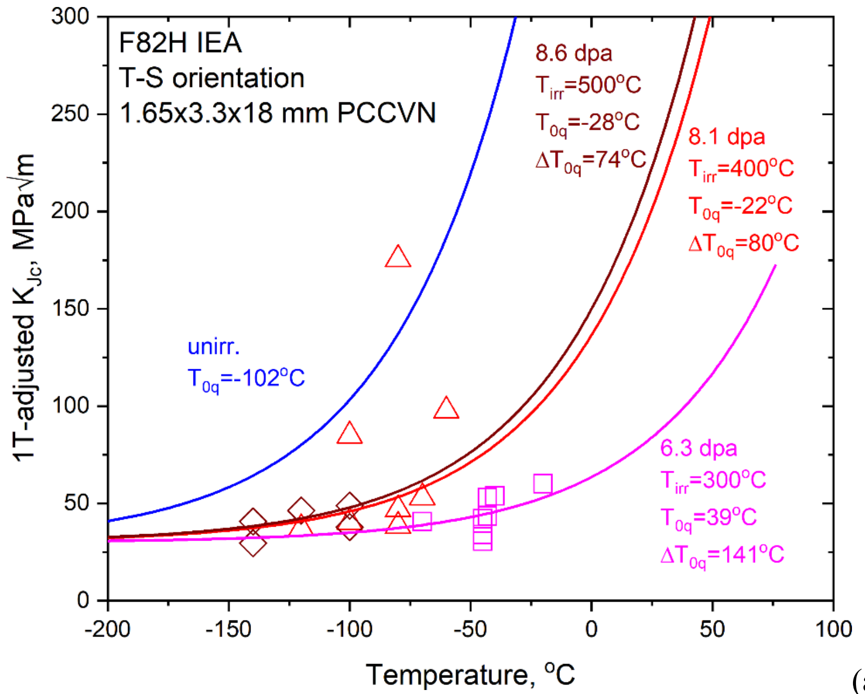

(a)

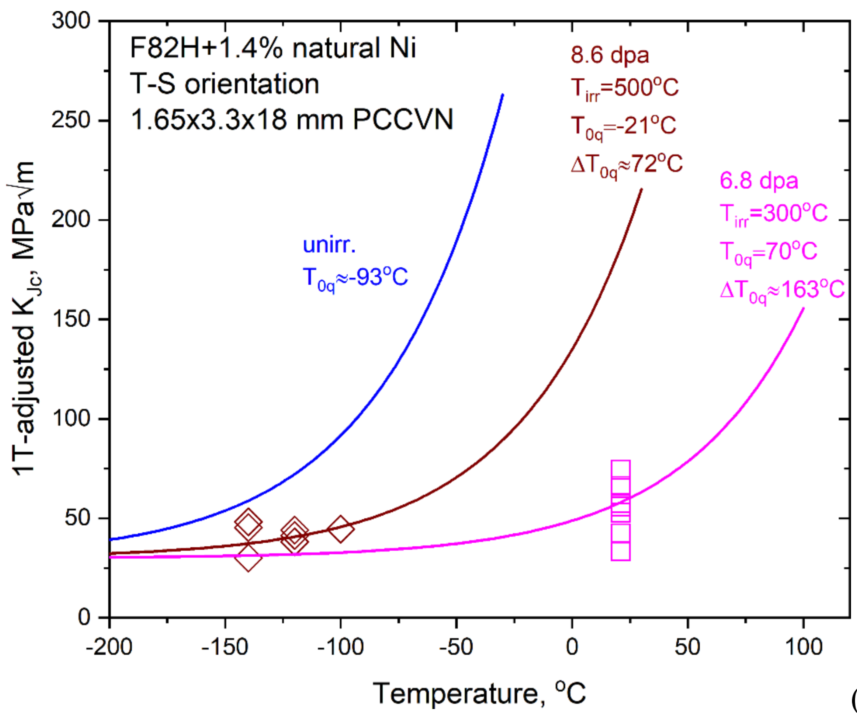

(b)

Figure 6 JP27 MC results for F82H IEA in (a), F82H Mod3 in (b), F82H+1.4% ^{58}Ni in (c), and F82H+1.4% ^{60}Ni in (d) [[38]

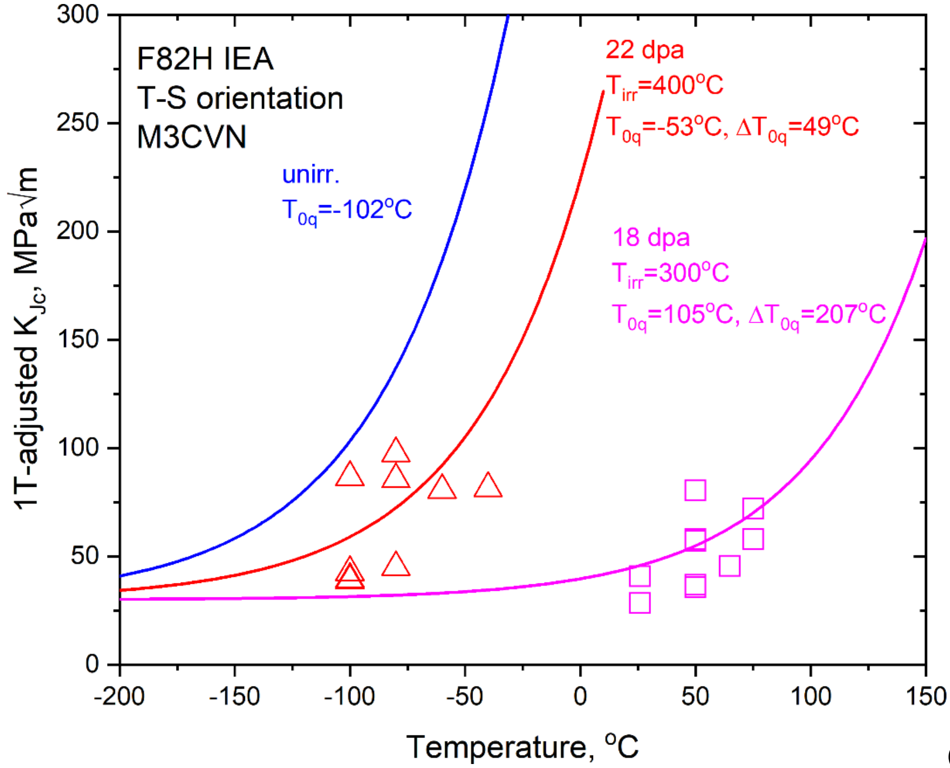

(a)

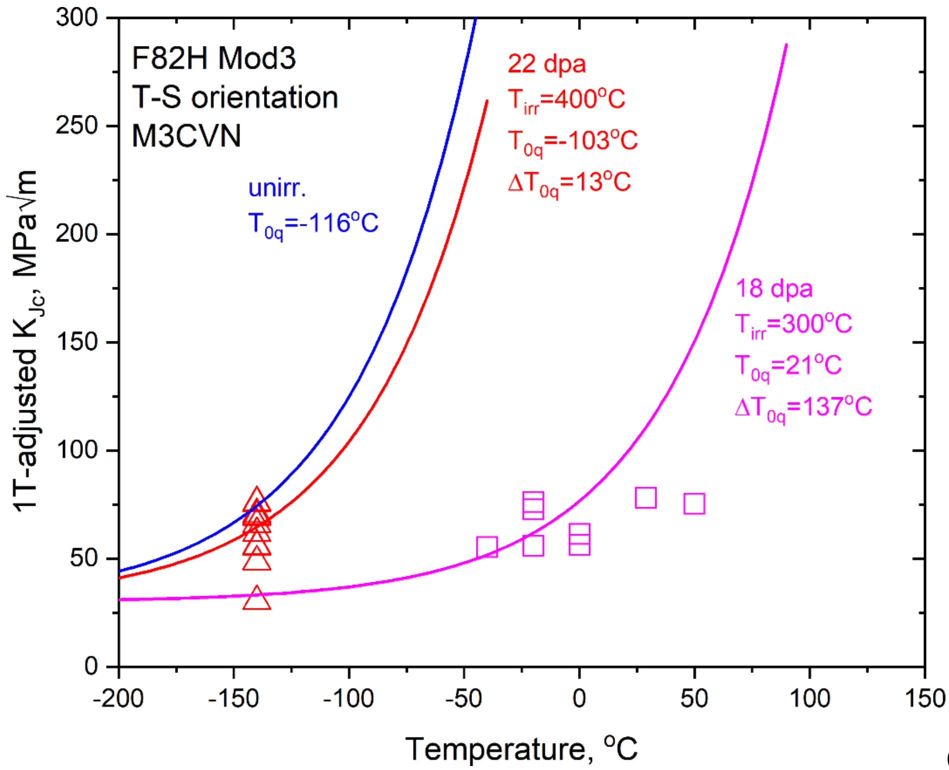

(b)

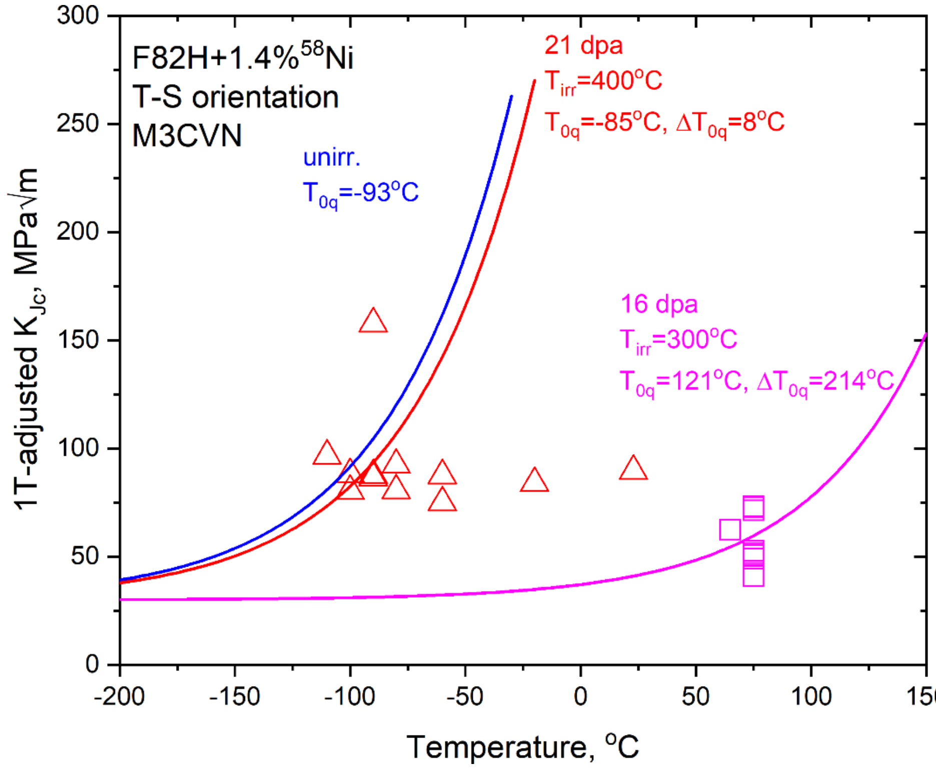
F82H+1.4%58Ni
T-S orientation
M3CVN
21 dpa
Tirr=400°C
T0q=-85°C, ΔT0q=8°C
unirr.
T0q=-93°C
16 dpa
Tirr=300°C
T0q=121°C, ΔT0q=214°C
1T-adjusted KJc, MPa√m
Temperature, °C
300
250
200
150
100
50
0
-200
-150
-100
-50
0
50
100
150
(c)

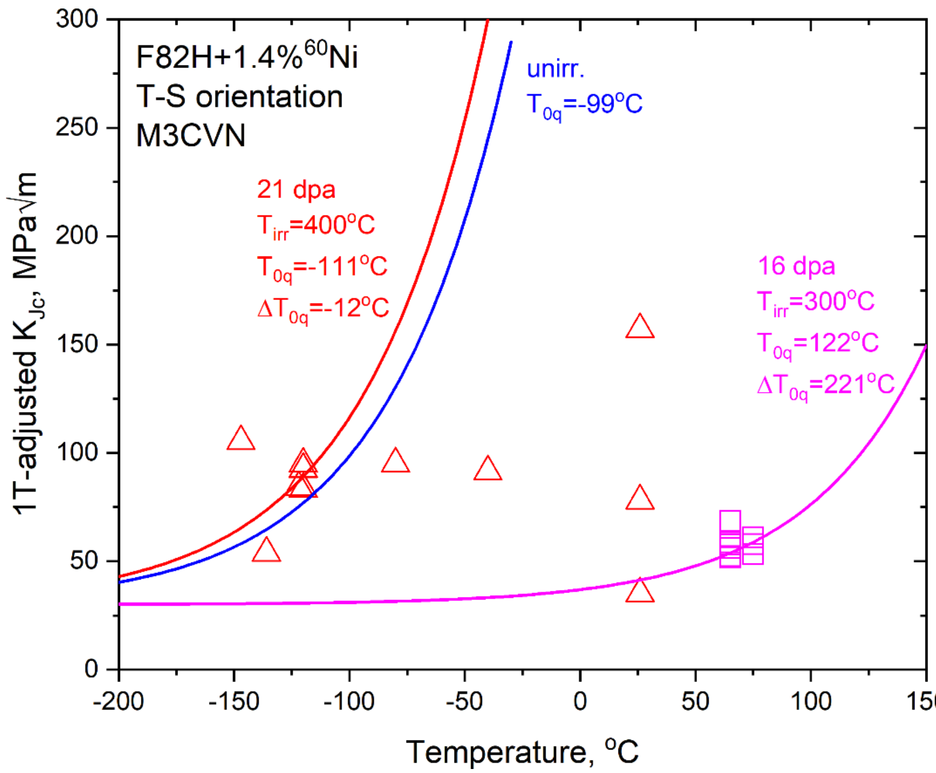
F82H+1.4%60Ni
T-S orientation
M3CVN
unirr.
T0q=-99°C
21 dpa
Tirr=400°C
T0q=-111°C
ΔT0q=-12°C
16 dpa
Tirr=300°C
T0q=122°C
ΔT0q=221°C
1T-adjusted KJc, MPa√m
Temperature, °C
300
250
200
150
100
50
0
-200
-150
-100
-50
0
50
100
150
(d)

Figure 7 JP28 and JP29 MC results for F82H IEA in (a), F82H Mod3 in (b), F82H+1.4% ^{58}Ni in (c), and F82H+1.4% ^{60}Ni in (d)

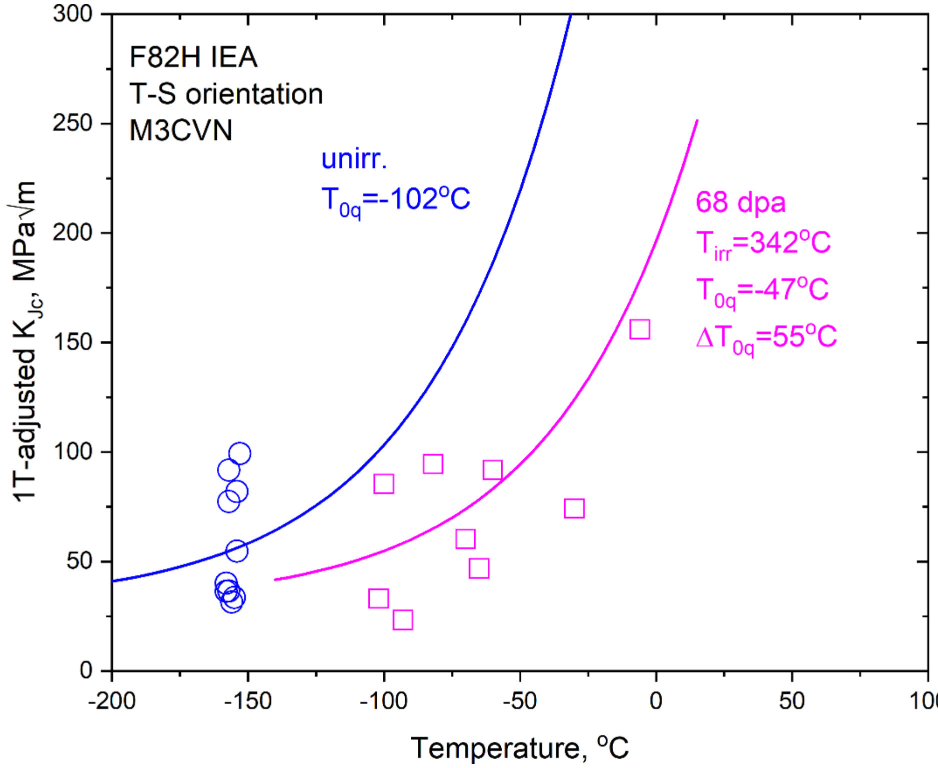

(a)

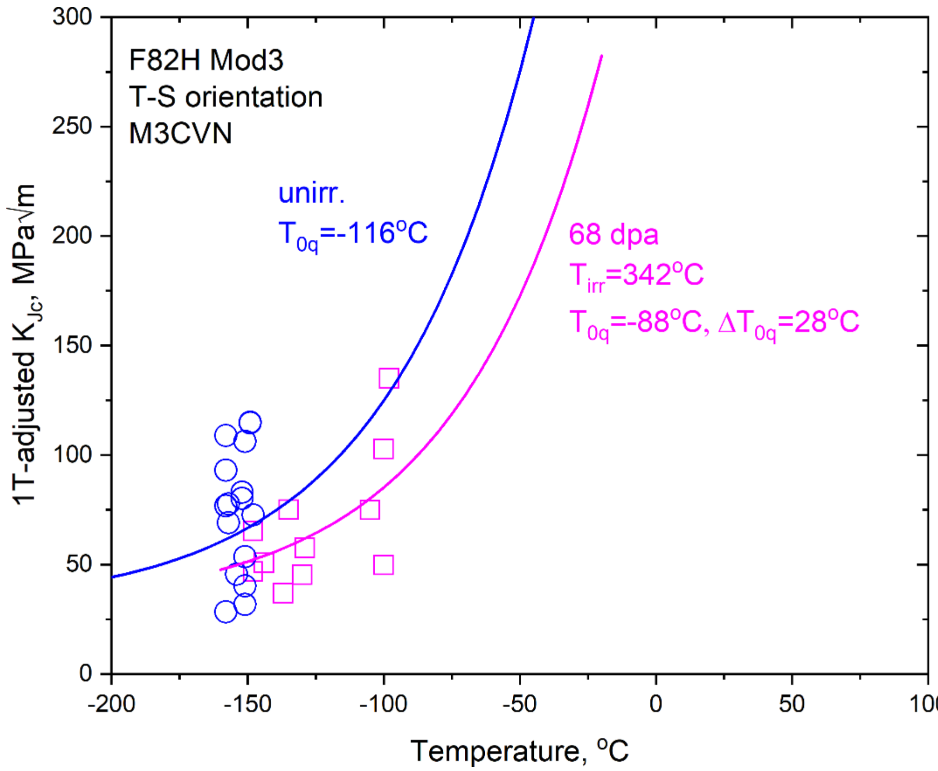

(b)

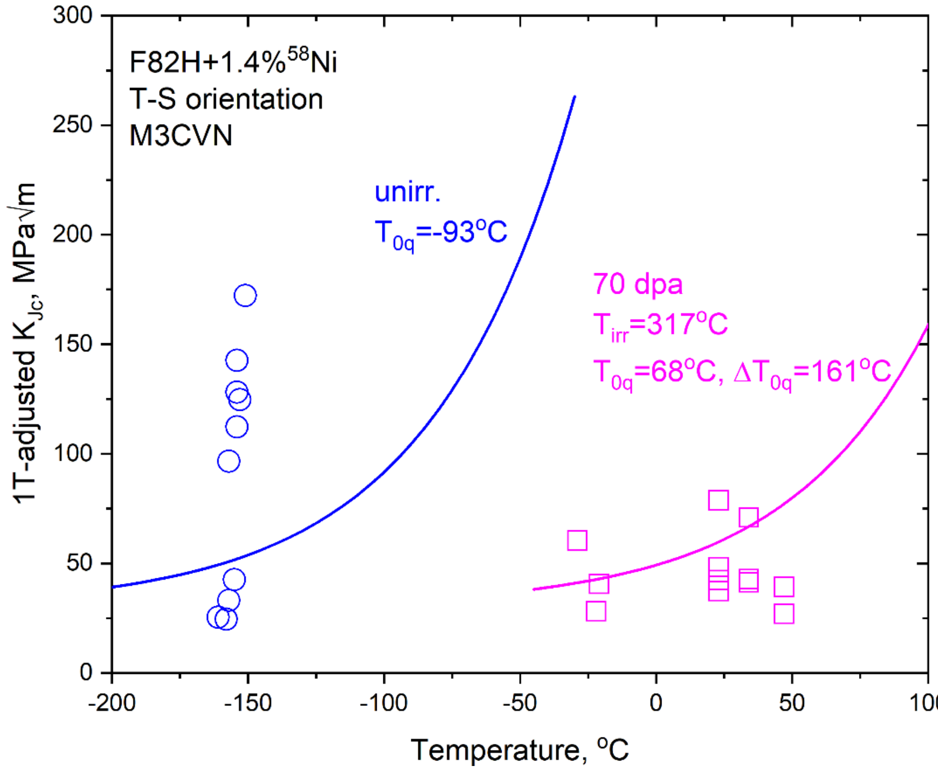
F82H+1.4%58Ni
T-S orientation
M3CVN
unirr.
T0q=-93oC
70 dpa
Tirr=317oC
T0q=68oC, ΔT0q=161oC
1T-adjusted KJc, MPa√m
Temperature, oC
300
250
200
150
100
50
0
-200
-150
-100
-50
0
50
100

(c)

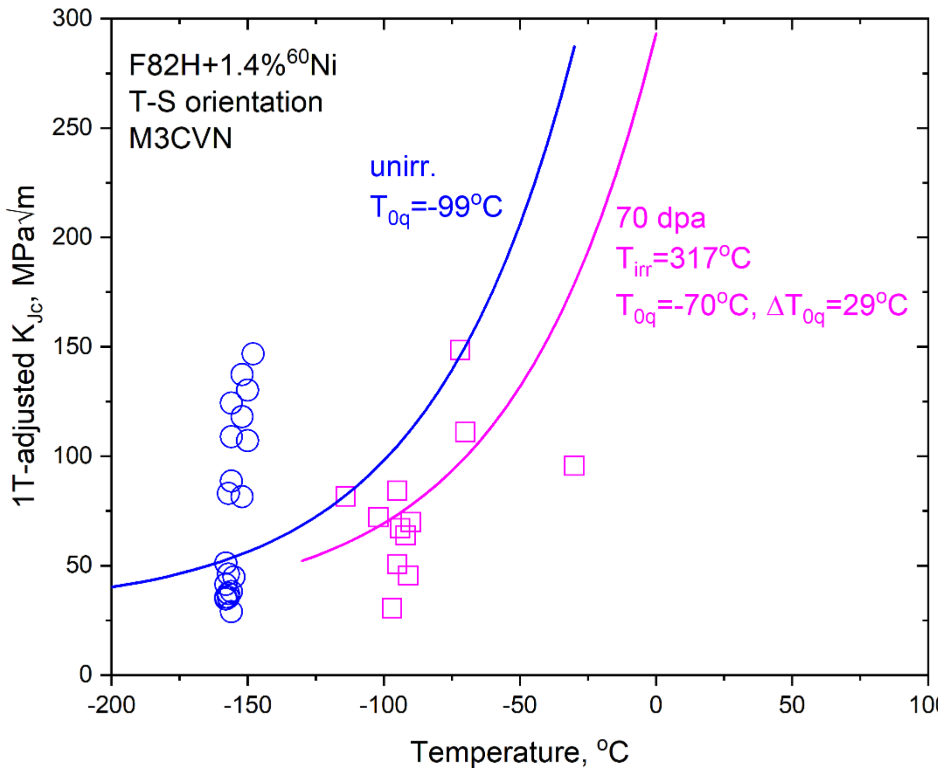
F82H+1.4%60Ni
T-S orientation
M3CVN
unirr.
T0q=-99oC
70 dpa
Tirr=317oC
T0q=-70oC, ΔT0q=29oC
1T-adjusted KJc, MPa√m
Temperature, oC
300
250
200
150
100
50
0
-200
-150
-100
-50
0
50
100

(d)

Figure 8 The effect of irradiation temperature and dose on the fracture toughness of F82H IEA and F82H Mod3

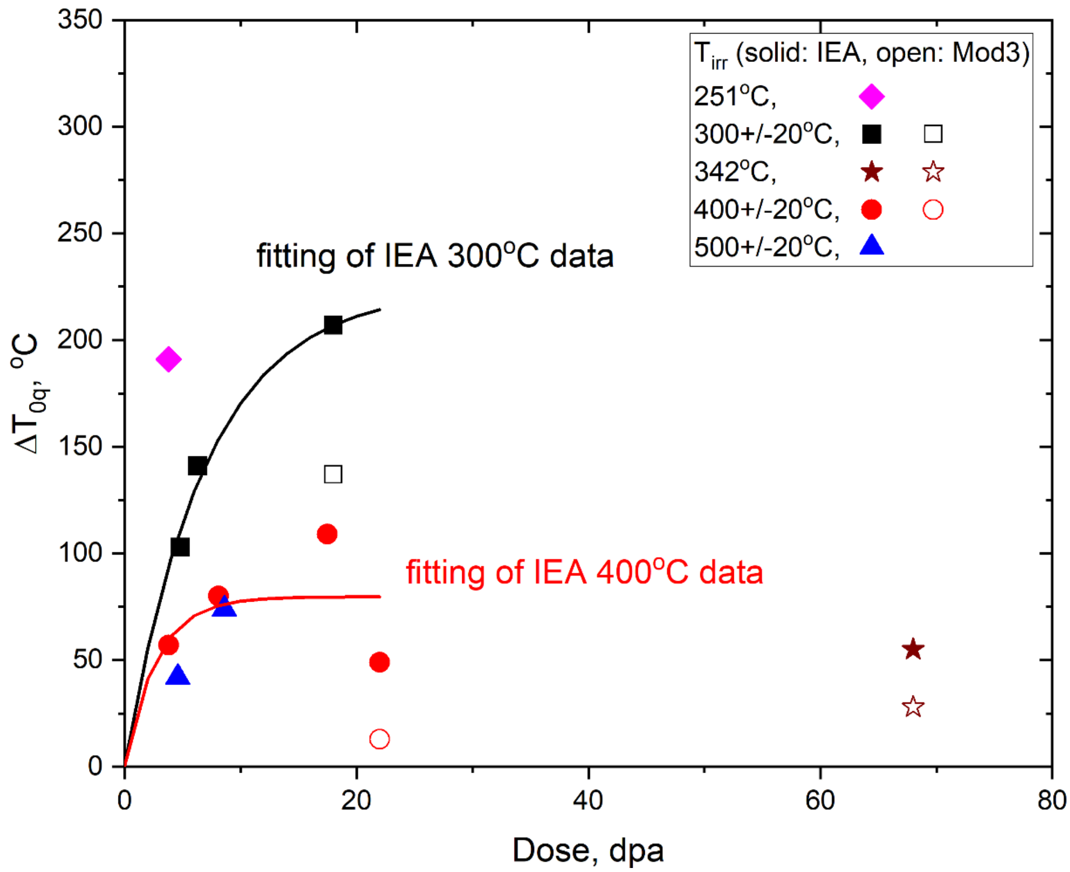

Figure 9 Comparison of irradiation embrittlement between JP27 and JP28/29 for F82H IEA, F82H Mod3, F82H+1.4% ^{58}Ni, and F82H+1.4% ^{60}Ni.

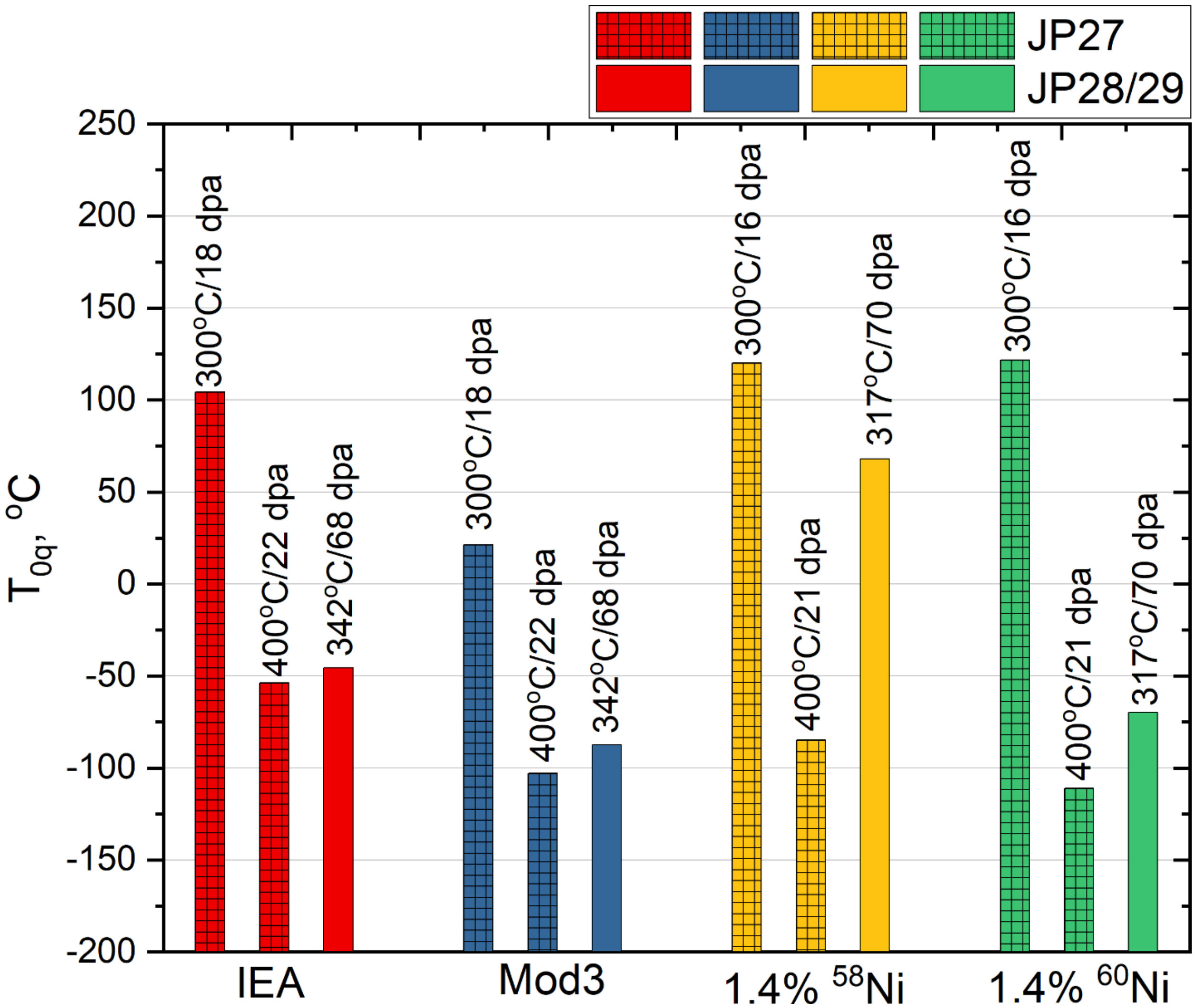

Figure 10 Comparison of irradiation embrittlement between this study and literature for F82H IEA and Eurofer97

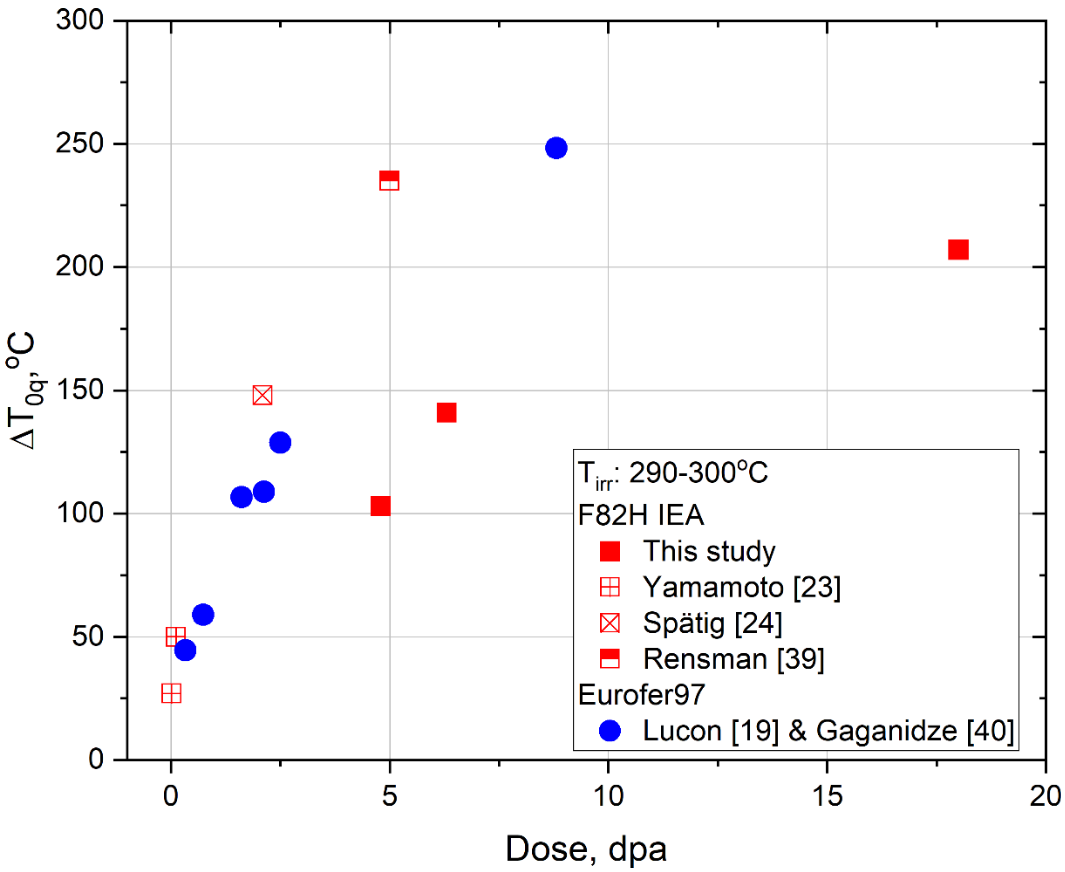

Figure 11 Comparison of the upward shift in the MC reference temperature T_0 between F82H IEA and Ni-doped F82H. Hatched histograms are used for the 68 dpa – 70 dpa irradiations due to uncertainties in the irradiation temperature for the high dose irradiation.

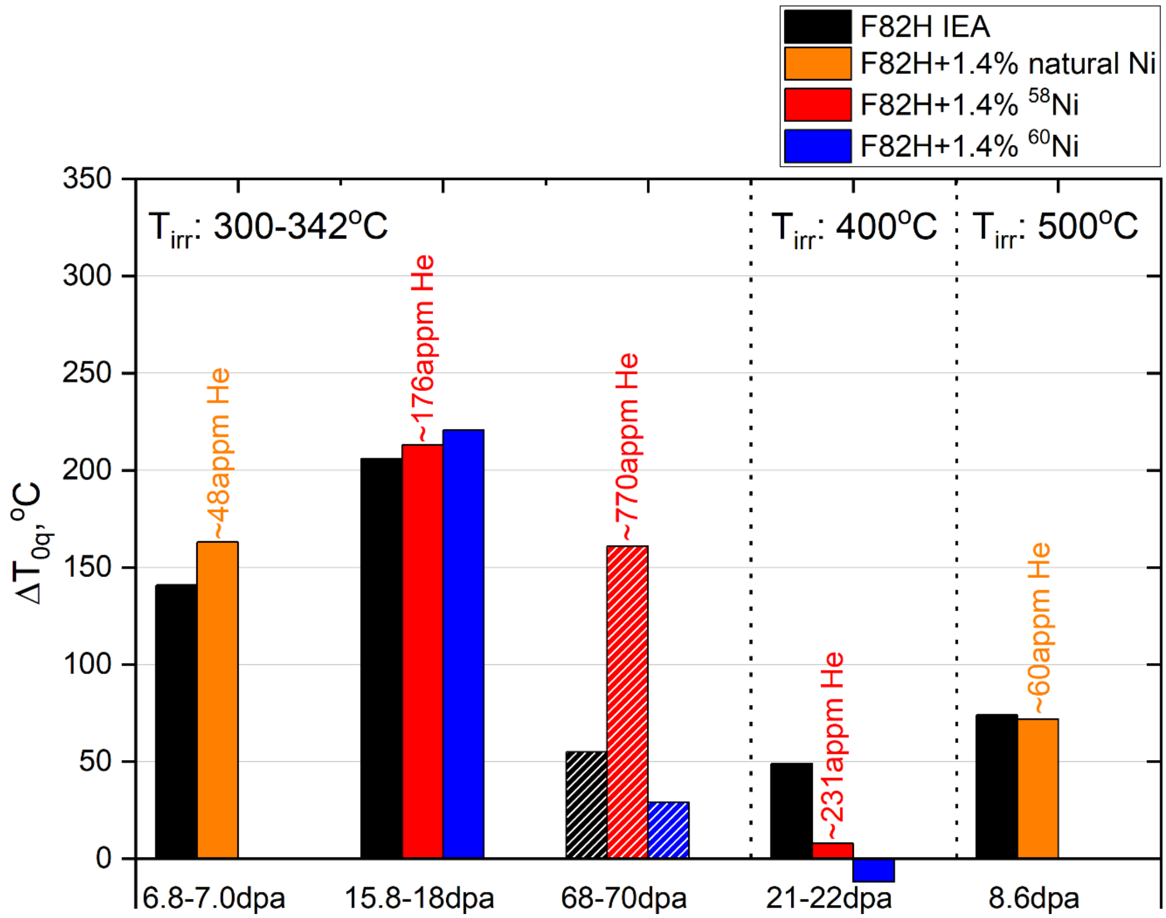

List of Tables

Table 1 Chemical composition of various F82H steels (wt%)

Alloys	Fe	Cr	W	V	Ta	C	Ti	Si	Mn	N	Ni
F82H IEA	Bal.	7.89	1.99	0.19	0.02	0.09	0.004	0.07	0.10	0.006	-
F82H Mod3	Bal.	8.16	1.94	0.20	0.092	0.10	<0.0001	0.10	0.13	0.0014	0.01
F82H+1.4% natural Ni	Bal.	7.82	1.98	0.31	0.021	0.072	<0.002	0.10	0.11	0.001	1.36
F82H+1.4% ^{58}Ni	Bal.	7.80	2.01	0.21	0.14	0.053	0.004	0.10	0.11	0.0013	1.32
F82H+1.4% ^{60}Ni	Bal.	7.75	2.03	0.19	0.138	0.054	0.004	0.11	0.10	0.0014	1.36

Table 2 Heat treatment conditions of various F82H steels

Alloys	Heat treatment
F82H IEA	1040 °C/40 mins/air cool + 750 °C /1 hr/air cool
F82H Mod3	1040 °C/30 mins/air cool + 740 °C /1.5 hrs/air cool
F82H+1.4% natural Ni	1040 °C/30 mins/air cool + 750 °C /1.5 hrs/air cool
F82H+1.4% ^{58}Ni	1040 °C/30 mins/air cool + 750 °C /1.5 hrs/air cool
F82H+1.4%^{60}Ni	1040 °C/30 mins/air cool + 750 °C /1.5 hrs/air cool

Table 3 Calculated helium production rates for various F82H steels irradiated in HFIR flux trap positions [[28, [30-[33].

Alloys	Helium production rate (appm He/dpa)
F82H IEA	0.3
F82H Mod3	0.3
F82H+1.4% natural Ni	7
F82H+1.4% ^{58}Ni	11
F82H+1.4%^{60}Ni	0.3